ICIC Express Letters
Volume **16**, Number **12**, December **2022**
 ISSN 1881-803X
pp. **1249–1258**

HORIZON DETECTION FOR UAV ATTITUDE BASED ON IMAGE PROCESSING APPROACH

Dyah Aruming Tyas[1,*], Ika Candradewi[1], Baskara[2]
Novelio Putra Indarto[1], Haikal Abdurrahman[1], Yohan Argha[1]
Bakhtiar Alldino Ardi Sumbodo[1] and Andi Dharmawan[1]

[1]Department of Computer Science and Electronics
Faculty of Mathematics and Natural Sciences
Universitas Gadjah Mada
Building C, 4th Floor, North Sekip, Bulaksumur, Yogyakarta 55281, Indonesia
{ ika.candradewi; b.alldino.as; Andi_dharmawan }@ugm.ac.id
{ novelio.p.i; haikalabdurrahman; yohanargha2020 }@mail.ugm.ac.id
*Corresponding author: dyah.aruming.t@ugm.ac.id

[2]Department of Computer Science and Engineering
Toyohashi University of Technology
1-1 Hibarigaoka, Tempaku-cho, Toyohashi, Aichi 441-8580, Japan
Baskara.zv@tut.jp

Received December 2021; accepted March 2022

Abstract. *The UAV must have the capability for automatic stabilization to maintain its position. Automatic stabilization estimates the roll and pitch angle that makes the UAV fully autonomous. We can use AI and computer vision technology for UAV stabilization. In this study, a horizon detection system will be designed to obtain data on the orientation of the UAV relative to the earth's horizon using AI and computer vision. We proposed a method to detect the horizon line with U-Net semantic segmentation, find the horizon line candidate using dilation and bitwise operation AND, and find the horizon line by linear regression equation. Based on the evaluation of the horizon line detection test on 2 test videos, the average IOU value for the segmentation of the land area is 0.96. For the horizon line, the root mean squared error (RMSE) value for the roll is 8.51 degrees and for pitch is 18.28%. The results of the semantic segmentation of the land area show a good performance.*
Keywords: Horizon detection, Semantic segmentation, UAV attitude, Roll, Pitch

1. **Introduction.** Unmanned aerial vehicles (UAVs) have developed rapidly in recent years. Many applications have been using UAVs to help humans work in various ways, such as scientists who collect research data and engineers who create integrated technologies such as aerial surveys, and objects [1]. A simple UAV should be able to do autonomous things like flying, hovering in the air, or navigating without input from the pilot. A UAV should also own the ability for automatic stabilization and maintaining position. Automatic stabilization estimates the roll and pitch angle that makes the UAV fully autonomous. The rapid development of AI and computer vision technology can now be used for UAV stabilization [2]. Based on image processing from the camera mounted on the UAV it can be used to estimate the attitude of the UAV. One way is to detect the horizon line. Based on the detected horizon line, roll and pitch angles can be determined to maintain the balance of the UAV.

Various previous studies have utilized horizon detection in several applications. Horizon line detection can benefit UAVs' obstacle detection and navigation systems. Several

DOI: 10.24507/icicel.16.12.1249

approaches that have been used to detect horizons are intensity-based clustering and k-means clustering [3], polarization-based segmentation [4], a combination of canny edges, hough detectors and particle swarm optimization (PSO) algorithms [5].

In [6], graph-based segmentation has carried out horizon line detection. The weight calculation of the edges and the merging criteria of related domains were modified. Then horizon line was extracted using line segment detector (LSD), clustering, Ransac and length-weighted average on the sky-ground boundary. Carrio et al. [7] proposed horizon detection on thermal images for attitude estimation. The methods they offered are the infinite horizon method and the ConvNet-based method. The two proposed methods are proven valid for UAV attitude estimation by providing root mean squared (RMS) errors below 1.7°. In the maritime industry, horizon detection is also carried out in marine zone video surveillance [8,9].

Semantic segmentation is the process of classifying each pixel of an image as a class label to understand the image on a per-pixel level. Semantic segmentation is an important stage for some applications, such as biomedical image segmentation [10] and autonomous driving [11]. Marcellino et al. [12] used U-Net++ as a semantic segmentation method for crowd counting and has a better mean squared error (MSE) than previous studies for ShanghaiTech Part A dataset. Gunawan et al. [13] used semantic segmentation of aerial imagery (SSAI) and SegNet models for road and building extraction. SegNet's performance, in this case, obtained better results than the SSAI model. Semantic segmentation can be applied to horizon line detection by distinguishing between the sky and the ground in the image obtained when the UAV is flying.

In this study, a horizon detection system will be designed to obtain data on the orientation of the UAV relative to the earth's horizon using AI and computer vision. This horizon detection system will be run on a single board computer (SBC). We propose calculating roll and pitch using a combination of the U-Net semantic segmentation method and digital image processing methods. The rest of this paper is organized as follows. Section 2 describes UAV platform, dataset and methods used in this paper. Section 3 describes the proposed horizon detection system. Section 4 describes the experiment and result of the proposed method. Finally, Section 5 presents the conclusion of this paper.

2. **Materials and Methods.** In this section, we present materials and methods that we use in this study.

2.1. **UAV platform.** Figure 1 shows the UAV platform. This UAV is also used in the video data retrieval process for the dataset. This UAV is made using a composite hard foam core material with a single tail boom configuration, high wing tapper, and conventional stabilizer.

FIGURE 1. UAV design (left); UAV platform (right)

2.2. **Dataset.** The flight of the vehicle to retrieve data is carried out several times and different weather conditions such as morning, afternoon, evening, sunny, and cloudy. Data acquisition takes video using a Raspi camera embedded in the unmanned aerial vehicle (UAV). The video will record the horizon line from takeoff to landing. The video will

be saved on Raspberry Pi. Then, the set of frames is labelled using Labelbox (https://labelbox.com/). The label is a segmentation of land and sky in each frame. The dataset used in this study consists of 2102 images measuring 480 × 480 pixels. Then the data is resized into a smaller size. The data will be divided into 1608 training data (80%) and 404 test data (20%). Figure 2 shows some examples of images in the dataset.

FIGURE 2. Dataset's sample images

In this study, ground truth was created manually and anotated as land area. Then do the border extraction to get the horizon line. The gradient and constant values of the horizon line are calculated from the horizon line. Based on the gradient values and horizon line constants, the roll and pitch values can be obtained as described in the roll and pitch calculation method section. The roll and pitch values will become the ground truth for this study's roll and pitch data.

2.3. **Methods.** The horizon detection system on the UAV aims to detect the horizon line to obtain data on the orientation of the UAV relative to the earth's horizon using AI and computer vision. This orientation data is expected to back up the IMU sensor and assist the control system on the UAV. This horizon detection system is run on an SBC connected to the flight controller. The SBC is also equipped with a camera and AI accelerator. Figure 3 shows block diagram of AI support. The horizon detection process is separated into four steps.

1) **Semantic segmentation.** Semantic segmentation is carried out on the input image taken from the camera facing the front of the UAV. Semantic segmentation aims to detect the position of the sky and ground in the image. This process is carried out using a U-Net-based deep learning algorithm that has previously been trained using a labelled dataset. U-Net was chosen because it provides more precise segmentation results in a small number of training sets and provides fast processing speed with relatively small input sizes [11]. This is in accordance with this study which uses a small dataset with a small image size and requires fast processing speed to detect the horizon line so that

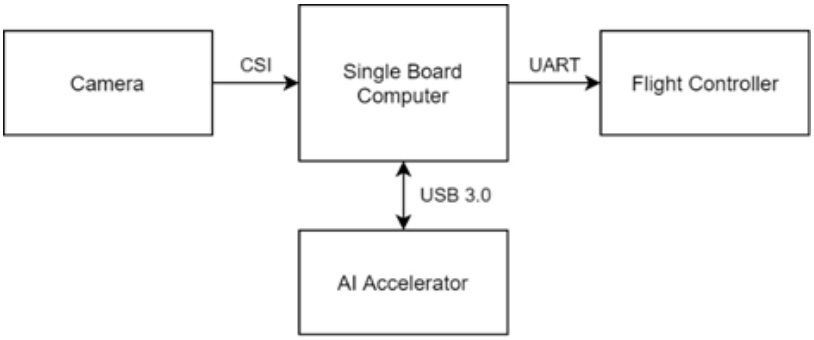

FIGURE 3. Block diagram of AI support

the UAV can automatically stabilize and maintain position. The training and testing processes are shown in Figure 4. The U-Net architecture training process is carried out to obtain an architectural model with a high IOU value. Furthermore, the architectural model is tested using data testing. If the IOU value obtained is less than 0.5, retraining is necessary. The output of this stage of a binary image shows the sky and the ground area (Figure 5).

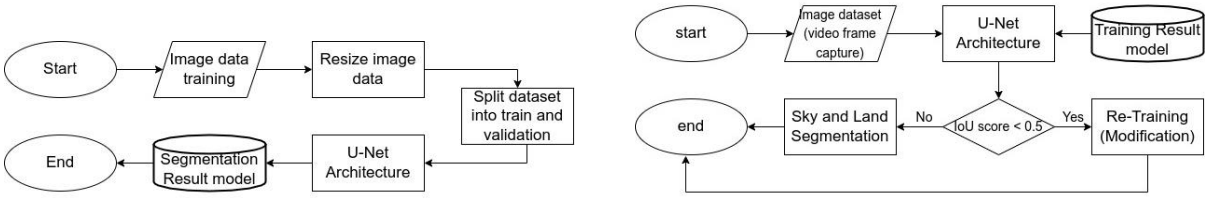

FIGURE 4. Training stage (left) and testing stage (right) of U-Net

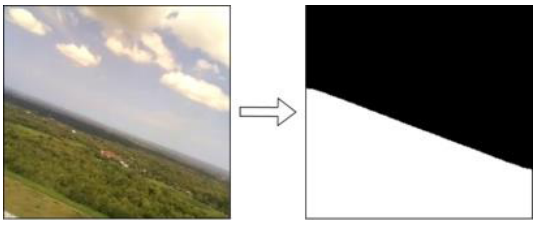

FIGURE 5. Semantic segmentation result

2) **Border extraction.** In the second stage, the boundary line between the sky and the ground is extracted using bitwise operations on the image. At this stage, dilation morphological operations are also performed to reduce noise in the image obtained in the semantic segmentation process. The output of this stage is a line that represents the horizon line in the image. Figure 6 shows the results of this stage.

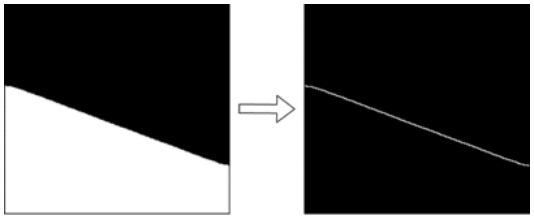

FIGURE 6. Border extraction result

3) **Linear regression.** In the third stage, linear regression is performed on the border extraction result to obtain the line equation. The line that has been obtained from the previous step is not straight, so it is necessary to do linear regression to get the slope (m) and constant (c), which will be used to calculate roll and pitch. The line formed from the previous process consists of a collection of pixels with specific coordinates. The pixel coordinate values are then used as input data to obtain a linear regression equation that matches the existing pixel distribution. Figure 7 shows the results of creating a regression line on the current border data.

4) **Roll and pitch calculation.** Roll and pitch measurements were carried out after obtaining border data from the linear regression stage. The measure aimed to ensure the UAV was always at the center of gravity of the horizon line. The UAV has degrees of freedom of movement in the air, consisting of the longitudinal, vertical and lateral axes. The meeting point of these axes is the CG (center of gravity) in the stability and manoeuvrability of the aircraft [14]. The manoeuvres include

(a) Rolling, the motion of the aircraft about the longitudinal axis using ailerons.
(b) Pitching, the movement of the aircraft about the lateral axis by using an elevator.
(c) Yawing, the movement of the aircraft about the vertical axis using the rudder.

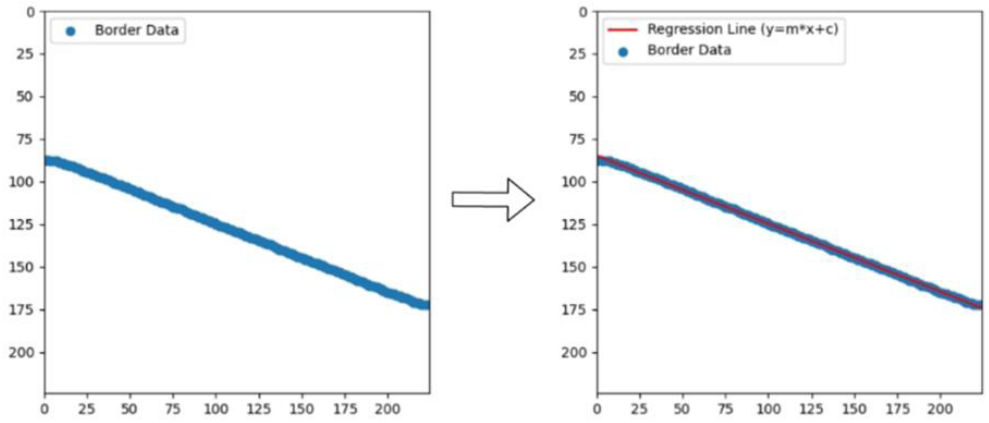

FIGURE 7. Horizon line from border data in regression linear stage

The calculation of roll and pitch used in this study uses the following approach:

- **Roll angle (α).** The roll angle is obtained using a trigonometric function. If we look at Figure 8, we can find the relation of trigonometric function ($y/x = \tan \alpha$), horizon line (m) and roll angle. So to find the roll angle, we can use $\alpha = y/x$. By using the slope-intercept form of a line ($y = mx + c$), we assume the value of $c = 0$ because the roll angle is not affected by the intercept, so we get $m = y/x$. If we substitute this equation to $\alpha = y/x$, we get $\alpha = m$.

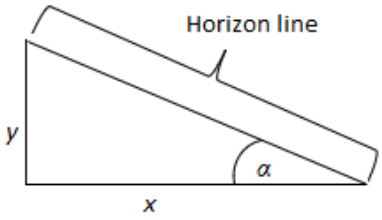

FIGURE 8. Illustration of the horizon line in the trigonometric plane

- **Pitch (θ).** The concept used in calculating the pitch is to calculate the position of the horizon line on the frame with width w and height h in the center point of the frame as the 0 point or reference point. Assume Figure 9 is a camera captured frame with a red line as the result of the detection of the horizon line and the blue dotted line being the center line of the frame. To get the pitch value, the midpoint of the frame is used, namely at the $w/2$ position in the horizon line equation. So it can be illustrated as Figure 9(c).

The equation $(m \cdot (w/2) + c)$ returns a value indicating the position of the horizon line. However, the position is not based on the reference point or the midpoint of the frame. So it is necessary to give an offset of $h/2$. Please note that the pitch angle will be positive if the aircraft is in a takeoff position (facing the sky) which makes the horizon line in the frame below the midpoint; otherwise, if the aircraft is in a landing (facing the ground) position the horizon line captured by the camera is above the middle point of the frame. So we need an offset equation that can adjust these conditions as shown in Equation (1) where y_{offset} is line equation with offsite. Figure 9(d) shows illustration after giving offset.

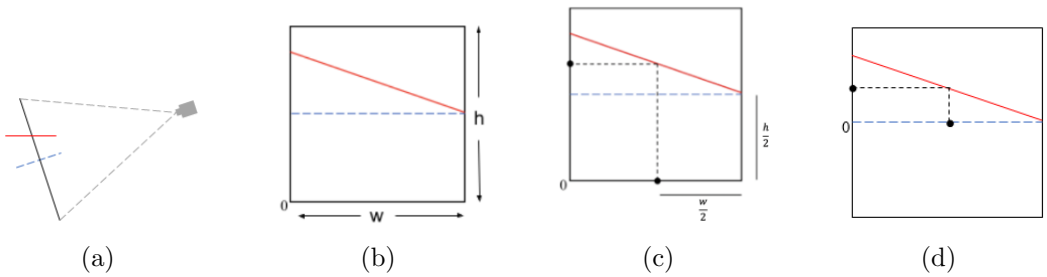

(a) (b) (c) (d)

FIGURE 9. (a) Illustration of a horizon line frame captured at the user's point of view; (b) the camera's point of view; (c) representation of the center point of the frame against the horizon line to get its position on the vertical axis; (d) giving offset to shift the value 0

Equation (1) still depends on the frame size, where the value will change if the frame size changes in different systems. So it is necessary to generalize so that it can be used on all systems with various frame sizes, by using a percent scale. The results of the previous equation will be divided by the frame size $h/2$ so that regardless of the frame size, the resulting pitch value will remain the same. Thus, the pitch value can be calculated by Equation (2), where θ is pitch value in percent, m is horizon line gradient, w is width of input image in pixel, h is height of input image in pixel and c is intercept horizon line.

$$y_{offset} = (m \cdot (w/2) + c) - h/2 \tag{1}$$

$$\theta = (y_{offset}/(h/2)) \times 100\% \tag{2}$$

2.4. **Evaluation matrix.** In the case of object detection, the evaluation metric used is to measure how close the detected bounding box is to the ground truth bounding box. The detection results are correct if the area and location of the ground-truth bounding box and prediction bounding box are the same. The result can be assessed using the intersection over union (IOU), a measurement based on the Jaccard index, a similarity coefficient for two sets of data [15]. Figure 10 shows an illustration of the IOU. IOU measurements were carried out in this study on the segmented land area and ground truth land area.

$$\text{IOU} = \frac{\text{area of overlap}}{\text{area of union}} =$$

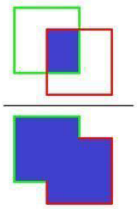

FIGURE 10. Illustration of the IOU [15]

3. **Horizon Detection System.** Figure 11 shows a flowchart of our proposed horizon line detection system for UAV. This diagram will not explain how the training process is carried out but will capture the horizon image after obtaining the training model. First, the system will load the training dataset model so that the system does not need to do training every time the program is run. Then the program must first access the camera to get the image. If the camera cannot be accessed, the program will stop and must be done to ensure no damage to any components used.

After the image from the camera is obtained, each frame will go through several stages before getting the horizon line. First, the structure will go through a preprocessing step where the size will be adjusted to the size of the dataset, change the colour space from BGR to RGB, and normalize. The results of the preprocessing frame will be predicted

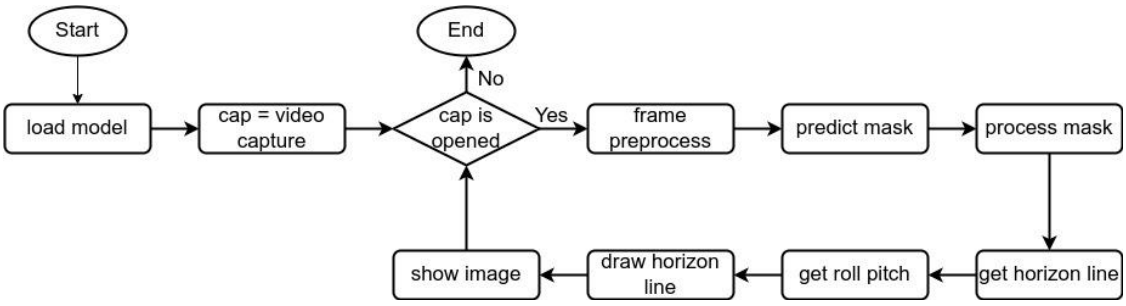

FIGURE 11. Horizon line detection system flowchart

FIGURE 12. The result of horizon line detection system

to obtain land and sky segmentation data. The two segmentation results will then be processed to get a line of intersection between them by a dilation process and a bitwise AND. A line of the corner will be obtained between the two segmentations.

Furthermore, linear regression is applied to obtaining slope (m) and constant (c), calculating roll and pitch. After the roll and pitch data is received, a line will be drawn on the frame and the two data to facilitate debugging (Figure 12). Then, the frame will be displayed on the screen. At the end of the system, the camera will capture the frame processed from the beginning. This process is carried out continuously until the program is terminated.

4. **Experiment and Result.** Making a model for segmentation is done by a training process. Three-way data process the dataset splits where the dataset is divided into test set, training set, and validation set. The training set and validation set are used at the model selection stage. The epoch value depends on the convergence process of the model, while the batch value is selected based on the value of the virtual ram, while the learning rate value is used as the default value 1. The image size used is 128 $\times$ 128 because the computation process is faster than 256 $\times$ 256, so the U-Net training process is carried out using some of the best parameters: epoch 50, batch size 32, learning rate 1. Figure 13 shows the training process results. The orange is the predicted output result, the blue is the training result, and the red is the validation result in the training phase. The condition is stable at the 50th epoch with accuracy above 95% (Figure 13(a)), in line with the slope of the loss value and the validation data depicted by the red line. The value is not far from the blue line, which results from the model evaluation of the training data, indicating that the model has converged because the test results on the validation data are close to the training results. The IOU value obtained from the training process reached 0.95 while the testing process got 0.98 caused by an imbalanced dataset. In the training data, there are more land classes than sky classes.

Horizon line detection result. The evaluation of the horizon line detection system was carried out using two new videos. The first video consists of 100 seconds, and the second

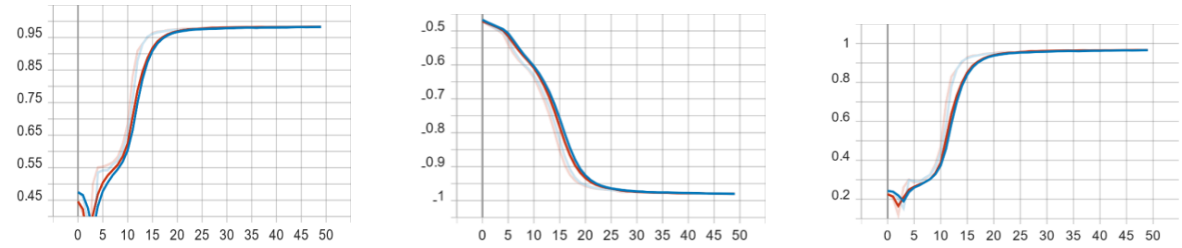

(a) Epoch vs accuracy training

(b) Epoch vs loss training

(c) Epoch vs max mean IOU training

FIGURE 13. (color online) Graph of training and validation results

TABLE 1. Result of IOU, RMSE roll and pitch

	IOU	RMSE roll (°)	RMSE pitch (%)
Video 1	0.96	13.78	26.06
Video 2	0.97	3.23	10.51
Average	0.96	8.51	18.28

video consists of 95 seconds. The evaluation process is carried out using images sampled every second. The first video consists of 100 seconds, and the second video consists of 95 seconds. So we have 100 images in the first video and 95 images from the second video. Table 1 shows the results of calculating the IOU, RMSE roll and RMSE pitch of the two videos. In the IOU calculation, the land area detected by the system is calculated with the actual land area. Based on the experimental results, the IOU value in the first video is 0.96 and the IOU value in the second video is 0.97. An average IOU value of 0.96 was obtained from the two test videos, which shows the results of the overlap area of the system and ground truth reaching 96%, which means the system can detect the ground area well.

The next stage is evaluating roll and pitch values based on the system's horizon line, which is compared with the ground truth roll and pitch values. Based on the experiment, the RMSE value from the roll calculation in the first video was 13.78°, while in the second video, it was 3.23°. The average RMSE roll of the two videos is 8.51°. The RMSE pitch calculation result from the first video is 26.06%, and the second video is 10.51%. The average RMSE pitch measurement of the two videos is 18.28%. The RMSE average value of roll and pitch is still quite significant, and this is because the horizon line generated by the system does not match the horizon line formed from the ground truth area of the land. The discrepancy comes from a linear regression process that creates a horizon line based on data from border extraction. Table 2 shows the comparison of the horizon line formed from the ground truth area of the land (green) and the predicted horizon line (red). In the first column in Table 2, it can be seen that the red horizon line is very different from the green horizon line. It is because in the segmentation process, trees are considered as land areas. The result will impact the suitability of the horizon line formed from the linear regression stage. In the second column in Table 2, a sample of the system horizon detection results (red) is shown close to the actual horizon line (green).

Figure 14 and Figure 15 show the predicted roll and pitch data from the system vs ground truth. From Figure 14, it can be seen that the prediction results for roll values are very volatile. In the graph, we can see the initial data in the middle of both roll and pitch. It can be seen that the prediction results (blue line) have a reasonably significant deviation from the actual roll and pitch values. The horizon candidate fails to process from a line with a border and next to the linear regression, which affects a more substantial proportion of the land area.

TABLE 2. (color online) Comparison of ground truth and horizon line prediction result

Sample 1	Sample 2
	

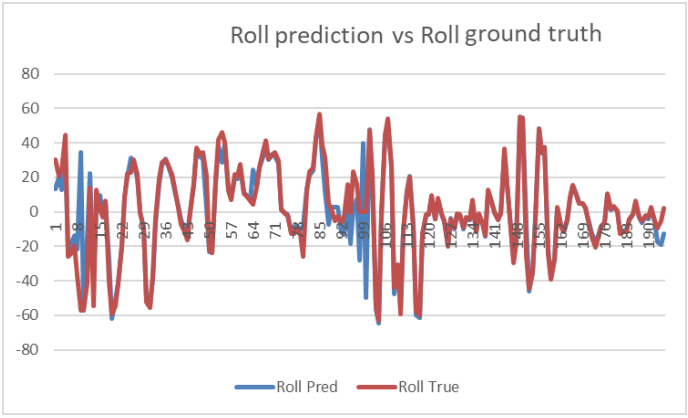

FIGURE 14. (color online) Comparison of roll prediction and ground truth

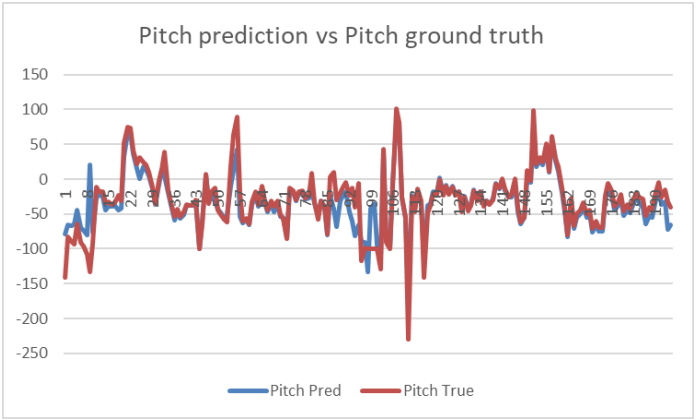

FIGURE 15. (color online) Comparison of pitch prediction and ground truth

5. **Conclusions.** Based on the results and discussions that have been obtained, we propose a method step to detect the horizon line. From the segmentation stage, the IOU value from the training process reaches 0.95 while the testing process gets 0.98. Furthermore, the results of both frames are post-processing dilation and bitwise operation AND in order to obtain a candidate horizon line. Furthermore, the candidate horizon line is processed by linear regression to obtain a horizon line. From the results of the horizon line detection test on the 2 test videos, the average IOU value for ground area segmentation is 0.96 and for the horizon line the RMSE value for roll is 8.51 degrees and for pitch is 18.28%. The roll and pitch calculation approach in the proposed method still needs to be developed to get a low error value for future research. In addition to future work, testing the calculation of the roll and pitch angle for the attitude UAV with image processing on the system can be compared with the results of the IMU sensor readings.

Acknowledgment. The authors would like to thank our team in Deep Learning Research Center Universitas Gadjah Mada for their support. This research is supported by the Faculty of Mathematics and Natural Sciences, Universitas Gadjah Mada and PT. Epsindo Prima Solusi collaborated on this project with matching funds from the Kedaireka Matching Fund for Higher Education, the Business World, and the Industrial World.

REFERENCES

[1] D. Giordan et al., The use of unmanned aerial vehicles (UAVs) for engineering geology applications, *Bulletin of Engineering Geology and the Environment*, vol.79, no.7, pp.3437-3481, DOI: 10.1007/s10064-020-01766-299, 2020.

[2] M. Javaid, A. Haleem, R. P. Singh, S. Rab and R. Suman, Exploring impact and features of machine vision for progressive industry 4.0 culture, *Sensors International*, vol.3, 100132, DOI: 10.1016/j.sintl.2021.100132, 2022.

[3] N. S. Borounjeni, S. A. Etemad and A. Whitehead, Robust horizon detection using segmentation for UAV applications, *The 9th Conference on Computer and Robot Vision*, Toronto, ON, Canada, pp.346-352, DOI: 10.1109/CRV.2012.52, 2012.

[4] A. E. R. Shabayek, C. Demonceaux, O. Morel and D. Fofi, Vision based UAV attitude estimation: Progress and insights, *Journal of Intelligent and Robotic Systems*, vol.65, nos.1-4, pp.295-308, DOI: 10.1007/s10846-011-9588-y, 2012.

[5] S. Timotheatos, S. Piperakis, A. Argyros and P. Trahanias, Vision based horizon detection for UAV navigation, in *Mechanisms and Machine Science*, Springrer, Cham, 2019.

[6] Y. Xu, H. Yan, Y. Ma and P. Guo, Graph-based horizon line detection for UAV navigation, *IEEE Journal of Selected Topics in Applied Earth Observations and Remote Sensing*, vol.14, pp.11683-11698, 2021.

[7] A. Carrio, H. Balve and P. Campoy, Attitude estimation using horizon detection in thermal images, *International Journal of Micro Air Vehicles*, vol.10, no.4, pp.352-361, DOI: 10.1177/1756829318804761, 2018.

[8] Y. Sun and L. Fu, Coarse-fine-stitched: A robust maritime horizon line detection method for unmanned surface vehicle applications, *Sensors*, vol.18, no.9, 2825, DOI: 10.3390/s18092825, 2018.

[9] C. Y. Jeong, H. S. Yang and K. D. Moon, Horizon detection in maritime images using scene parsing network, *Electronics Letters*, vol.54, no.12, pp.760-762, DOI: 10.1049/el.2018.0989, 2018.

[10] O. Ronneberger, P. Fischer and T. Brox, U-Net: Convolutional networks for biomedical image segmentation, *Medical Image Computing and Computer-Assisted Intervention – MICCAI 2015, Lecture Notes in Computer Science*, vol.9351, Springer, Cham, 2015.

[11] L. A. Tran and M. H. Le, Robust U-Net-based road lane markings detection for autonomous driving, *2019 International Conference on System Science and Engineering (ICSSE)*, Dong Hoi, Vietnam, pp.62-66, DOI: 10.1109/ICSSE.2019.8823532, 2019.

[12] Marcellino, T. W. Cenggoro and B. Pardamean, UNet++ with scale pyramid for crowd counting, *ICIC Express Letters*, vol.16, no.1, pp.75-82, DOI: 10.24507/icicel.16.01.75, 2022.

[13] A. A. S. Gunawan, I. Arifiany and E. Irwansyah, Semantic segmentation of aerial imagery for road and building extraction with deep learning, *ICIC Express Letters*, vol.14, no.1, pp.43-51, DOI: 10.24507/icicel.14.01.43, 2020.

[14] R. Hidayat and R. Mardiyanto, Development of automatic navigation system on UAV (Unmmanned Aerial Vehicle) with GPS (Global Positioning System) waypoint, *Jurnal Teknik ITS*, vol.5, no.2, pp.A898-A903, 2016.

[15] R. Padilla, W. L. Passos, T. L. B. Dias, S. L. Netto and E. A. B. Silva, A comparative analysis of object detection metrics with a companion open-source toolkit, *Electronics*, vol.10, no.3, 279, DOI: 10.3390/electronics10030279, 2021.